Prediction of In Vivo Rat Biliary Drug Clearance from an In Vitro Hepatocyte Efflux Model

Article *in* Drug Metabolism and Disposition: the Biological Fate of Chemicals · January 2014

DOI: 10.1124/dmd.113.054155 · Source: PubMed

9 authors, including:

Patrik Lundquist
Uppsala University
22 PUBLICATIONS **891** CITATIONS
SEE PROFILE

Urban Fagerholm
Södertörn University
38 PUBLICATIONS **2,000** CITATIONS
SEE PROFILE

Janet Hoogstraate
Valneva Sweden
28 PUBLICATIONS **908** CITATIONS
SEE PROFILE

Lovisa Afzelius
Pfizer
18 PUBLICATIONS **903** CITATIONS
SEE PROFILE

1521-009X/42/3/459–468$25.00
Drug Metabolism and Disposition
http://dx.doi.org/10.1124/dmd.113.054155
Drug Metab Dispos 42:459–468, March 2014

Prediction of In Vivo Rat Biliary Drug Clearance from an In Vitro Hepatocyte Efflux Model[S]

Patrik Lundquist, Johan Lööf, Urban Fagerholm, Ingemo Sjögren, Jenny Johansson, Sveinn Briem, Janet Hoogstraate, Lovisa Afzelius, and Tommy B. Andersson

CNS and Pain Innovative Medicines DMPK, AstraZeneca R&D, Södertälje (P.L., J.L., U.F., I.S., J.J., S.B., J.H., L.A.); Cardiovascular and Metabolic Diseases Innovative Medicines DMPK, AstraZeneca R&D, Mölndal (P.L., T.B.A.); Department of Pharmacy, Uppsala University, Uppsala (P.L.); and Section of Pharmacogenetics, Department of Physiology and Pharmacology, Karolinska Institutet, Stockholm (T.B.A.), Sweden

Received August 9, 2013; accepted January 6, 2014

ABSTRACT

Well-established techniques are available to predict in vivo hepatic uptake and metabolism from in vitro data, but predictive models for biliary clearance remain elusive. Several studies have verified the expression and activity of ATP-binding cassette (ABC) efflux transporters central to biliary clearance in freshly isolated rat hepatocytes, raising the possibility of predicting biliary clearance from in vitro efflux measurements. In the present study, short-term plated rat hepatocytes were evaluated as a model to predict biliary clearance from in vitro efflux measurements before major changes in transporter expression known to take place in long-term hepatocyte cultures. The short-term cultures were carefully characterized for their uptake and metabolic properties using a set of model compounds. In vitro efflux was studied using digoxin, fexofenadine, napsagatran, and rosuvastatin, representing compounds with over 100-fold differences in efflux rates in vitro and 60-fold difference in measured in vivo biliary clearance. The predicted biliary clearances from short-term plated rat hepatocytes were within 2-fold of measured in vivo values. As in vitro efflux includes both basolateral and canalicular effluxes, pronounced basolateral efflux may introduce errors in predictions for some compounds. In addition, in vitro rat hepatocyte uptake rates corrected for simultaneous efflux predicted rat in vivo hepatic clearance of the biliary cleared compounds with less than 2-fold error. Short-term plated hepatocytes could thus be used to quantify hepatocyte uptake, metabolism, and efflux of compounds and considerably improve the prediction of hepatic clearance, especially for compounds with a large biliary clearance component.

Introduction

Transport processes such as hepatic uptake or biliary efflux are central to the clearance (CL) of many drug compounds (Giacomini et al., 2010). Hepatic drug metabolism is performed by enzymes commonly divided into phase I enzymes (mainly cytochrome P450, P450) and phase II enzymes (conjugating enzymes such as UDP-glucoronosyltransferase, UGT). A special challenge is to predict the in vivo pharmacokinetics (PK) of compounds that are subject to a combination of uptake, metabolism, and efflux (Li et al., 2010).

Today, several techniques for investigation of hepatocyte uptake and metabolism of drug molecules are available, such as metabolic stability or uptake measurements using suspended hepatocytes (Soars et al., 2007). However, because isolated hepatocytes lose their tissue geometry, active efflux and biliary secretion of compounds are properties difficult to study in vitro (Li et al., 2010; De Bruyn et al., 2013). Robust in vitro models that also reflect biliary efflux in addition to hepatic uptake and metabolism would be valuable tools to evaluate drug disposition as well as the in vitro to in vivo extrapolation (IVIVE) of hepatic clearance. Compounds actively cleared by biliary or renal secretion belong in general to classes III and IV of the Biopharmaceutics Drug Disposition Classification System (BDDCS) proposed by Wu and Benet (2005). These classes are characterized by low metabolism, low permeability, and large transporter effects. Classes I and II are characterized by high metabolism and permeability and small transporter effects.

Sandwich-cultured hepatocytes (SCH) are a convenient in vitro model to use for biliary clearance studies because the hepatocytes after 4 to 5 days of culture develop a rudimentary canalicular network and polarized membrane expression of many transporters. The excretion of compounds into the canalicular compartment is used to calculate the biliary excretion (Liu et al., 1999; De Bruyn et al., 2013). This strategy has been successful in predicting the bile efflux of several drugs, but as noted by Li et al. (2010) and others, it often underpredicts biliary clearance by 10-fold to 100-fold (Nakakariya et al., 2012; De Bruyn et al., 2013). Partly this may be due to the down-regulation of both

dx.doi.org/10.1124/dmd.113.054155.
[S]This article has supplemental material available at dmd.aspetjournals.org.

ABBREVIATIONS: ABC, ATP-binding cassette; ACN, acetonitrile; AUC, area under the concentration-time curve; BCRP, breast cancer resistance protein; BDDCS, Biopharmaceutics Drug Disposition Classification System; C_{blood}/C_{plasma}, blood-to-plasma concentration ratio; CL, clearance; CL_{int}, intrinsic clearance; DMSO, dimethylsulfoxide; $f_{hepatic}$, the hepatically cleared fraction; FTC, fumitremorgin C; *fu*, fraction unbound, free fraction; GF120918, elacridar, *N*-4-[2-(1,2,3,4-tetrahydro-6,7-dimethoxy-2-isoquinolinyl)ethyl]-phenyl)-9,10-dihydro-5-methoxy-9-oxo-4-acridine carboxamide hydrochloride; h, as prefix, human; IVIVE, in vitro to in vivo extrapolation; KHL, Krebs-Henseleit buffer supplemented with 10 mM Hepes, pH 7.4; LC-MS/MS, liquid chromatography tandem mass spectrometry; MRP, multidrug resistance-associated protein; NTCP, Na^+-taurocholate cotransporting polypeptide; OATP, organic anion transporting polypeptide; OST, organic solute transporter; P450, Cytochrome P450; P-gp, P-glycoprotein; PK, pharmacokinetic; $Q_{h,\,b}$, hepatic blood flow; r, as prefix, rat; SCH, sandwich-cultured hepatocytes; UGT, UDP-glucoronosyltransferase; WE, William's E medium.

drug uptake and efflux transporters that has been demonstrated to take place within the first days after the plating of hepatocytes from both rats and humans (Liu et al., 1998; Li et al., 2009a; Kotani et al., 2011; Tchaparian et al., 2011; Kimoto et al., 2012; De Bruyn et al., 2013). Sinusoidal efflux transporters, such as rat multidrug resistance-associated protein 3 (rMRP3) and rat organic solute transporter α–organic solute transporter β (rOSTα-OSTβ) show low expression levels in normal livers but are up-regulated in cholestasis (Rippin et al., 2001; Luttringer et al., 2002; Boyer et al., 2006). The expression levels of rMRP4 and rMRP3 in rat liver, primary hepatocytes, and short-term cultures are low, but they are extensively up-regulated in longer term cultures (Rippin et al., 2001; Luttringer et al., 2002; Tchaparian et al., 2011). In addition the activity of many P450 enzymes is considerably reduced in SCH (De Bruyn et al., 2013). To compensate for expression changes in SCH, proteomics-based correction factors have been used with some success, but these are difficult to implement when the transporters involved in the disposition of a compound are not known (Li et al., 2010).

The fate of canalicular ATP-binding cassette (ABC) efflux transporters central to biliary excretion such as P-glycoprotein (P-gp), breast cancer resistance protein (BCRP), and multidrug resistance protein-2 (MRP2) in isolated hepatocytes has been debated. Some reports suggest that isolated rat hepatocytes lose part of their ABC transporters (Bow et al., 2008). Others studies have demonstrated both expression and activity of rP-gp, rBCRP, and rMRP2 in freshly isolated rat hepatocytes (Lam et al., 2006; Li et al., 2008, 2009a,b; Lundquist et al., 2014a). The retained activity of canalicular efflux transporters in primary rat hepatocytes demonstrated by these investigators raises the possibility of predicting biliary clearance from in vitro efflux measurements.

Short-term cultures may be a reliable in vitro model for studies on drug disposition as changes in hepatocyte transporter and drug metabolizing enzyme expression and activity are minor after 4 to 6 hours of culture (Jigorel et al., 2005; Beigel et al., 2008; Tchaparian et al., 2011).

In our present study, short-term cultures were demonstrated to be a robust model to predict the biliary clearance of a set of compounds with a large range of biliary clearances in vivo. Predictions were within 2-fold of measured biliary clearances, which is a considerable improvement compared with published methods. In addition, uptake and metabolic clearances were evaluated using short-term plated hepatocytes, and the results indicate that the model provides the possibility of assessing uptake, metabolic and efflux clearances.

Material and Methods

Nomenclature. This article, as recommended by Hagenbuch and Stieger (2013), for transporter nomenclature follows the gene and protein nomenclature guidelines of the HUGO Gene Nomenclature Committee (Gray et al., 2013) and the International Committee for Standardized Genetic Nomenclature in Mice (http://www.informatics.jax.org/mgihome/nomen/2009_gene.shtml) (2009). Protein names for both human and rodent proteins are written in capital letters (e.g., BCRP). In the interest of clarity human protein names are prefixed with h, and rat proteins are prefixed r (e.g., hBCRP, rBCRP). Protein names without prefix refer to the protein in general, not belonging to any particular species (e.g., a BCRP inhibitor).

Chemicals. Chemicals were purchased from Sigma-Aldrich (St. Louis, MO) unless otherwise specified.

Animals. Male Sprague-Dawley rats were acquired from Harlan Laboratories B.V. (Venray, the Netherlands). Rats were housed up to three per cage with free access to food and water. All animals were acclimatized for 2 weeks before the studies. All animal experiments were approved by the local animal ethics committee (Stockholms Södra djurförsöksetiska nämnd) and were conducted in compliance with national guidelines for the care and use of laboratory animals.

Preparation of Rat Hepatocytes. Rat hepatocytes were isolated according to a modified collagenase perfusion method previously described elsewhere (Bissell and Guzelian, 1980) from 7- to 8-week-old male Sprague-Dawley rats that were anesthetized with isoflurane (Abbott Scandinavia AB, Kista, Sweden). Shortly afterward, the liver was perfused in situ, first with 37°C calcium-free William's E (WE) medium containing 0.5 M EGTA, followed by WE medium, 10 mM HEPES (GIBCO/Life Technologies, Paisley, United Kingdom), pH 7.4, supplemented with 0.16 mg/ml collagenase type XI. The suspension of released hepatocytes was filtered through gauze, repeatedly centrifuged at 50*g* for 2 minutes, followed by aspiration of supernatant and resuspension of the pellet in WE, 10 mM HEPES, pH 7.4. Cell number and viability were determined using the Trypan blue exclusion method. Viability typically exceeded 90%. Cell preparations with viability of <80% were discarded.

Uptake and Metabolism Measurements of Test Compound with Plated Rat Hepatocytes and Suspended Cells. We seeded 0.75 million cells from a suspension of 10^6 cells/ml in culture medium [WE supplemented with 10 mM HEPES, pH 7.4, 10% fetal calf serum, 2 mM glutamine, and 0.01% insulin-transferrin-selenium A solution (GIBCO)] into each well of collagen I–coated 12-well plates (Biocoat; BD Biosciences, Franklin Lakes, NJ). The cells were incubated at room temperature for 10 minutes and were then left to attach to the plates for 90 minutes at 37°C in 5% CO_2. The plates were washed three times in 37°C Krebs-Henseleit buffer with 10 mM HEPES (GIBCO) pH 7.4 (KHL). Cells were preincubated in KHL at 37°C for 10 minutes before each experiment.

To start the uptake, KHL was removed, and 300 μl of 1 μM of test compound diluted in KHL and containing 0.1% dimethylsulfoxide (DMSO) was added to each well. Each time point was measured in triplicate. To stop the uptake reaction, 200 μl buffer from each well was transferred to a 96-well plate containing 300 μl of stop solution of acetonitrile (ACN) with 200 nM Warfarin (internal standard). The remaining buffer was removed, and the wells were washed twice in ice-cold KHL. The cell layer in washed wells was lysed with 300 μl of lysis solution, 2 parts of stop solution, and 1 part KHL with 200 nM warfarin. The lysates were incubated on ice for at least 10 minutes, then mixed and centrifuged at 1200*g* for 10 minutes. Before analysis, each fraction was diluted in KHL to contain 25% ACN. All samples were analyzed by liquid chromatography coupled with tandem mass spectrometry (LC-MS/MS). Binding was measured in empty plates and subtracted from the uptake measurements.

The activity of drug phase I and II metabolizing enzymes in rat hepatocytes in suspension and attached to plates was compared using a cocktail containing substrates for several CYP and phase II enzymes: 7-hydroxycoumarin (UGT), bufuralol (CYP2D2), diazepam (CYP2C11), diclofenac (CYP2C6), midazolam (CYP3A), and phenacetin (CYP1A2), each at 2 μM final concentration (isoform specificities from Kobayashi et al., 2002). Hepatocytes in suspension (10^6/ml) in KHL were incubated with the cocktail for 0 to 90 minutes. Samples were precipitated with 2 volumes of stop solution. Cells attached to plates were processed as was described for the uptake experiments.

For comparative purposes in IVIVE, the metabolic stability in rat liver microsomes was determined as described by Sohlenius-Sternbeck et al. (2010).

To test uptake activity in suspended and plated rat hepatocytes, five well-characterized uptake transporter substrates (atorvastatin, bosentan, estrone-3-sulfate, fexofenadine, and montelukast) and two passively transported substrates (atenolol and metoprolol; AstraZeneca) were tested. Experiments in plated cells were performed as described previously. The uptake measurements in suspended cells were performed using the media loss technique described by Soars et al. (2007).

To further investigate active transport in plated cells, atorvastatin uptake measurements were performed in the absence and presence of 2 μM of the organic anion transporting polypeptide (OATP) inhibitor cyclosporine A. The activity of Na^+-taurocholate cotransporting polypeptide (NTCP) in plated cells was studied by comparing the uptake of taurocholate in sodium-containing buffer and sodium-free buffer, substituted with equimolar choline. The influence of temperature on passive uptake in plated rat hepatocytes was investigated using the passively uptaken substrate atenolol at 37°C and 4°C.

In Vitro Efflux Measurements. Four compounds with complete human in vivo PK were identified: digoxin, napsagatran, fexofenadine, and rosuvastatin. Napsagatran was a kind gift from Hoffman-La Roche, Basel, Switzerland. Inclusion criteria were plasma clearance (CL_{plasma}) and biliary clearance (CL_{bile}) measured after intravenous administration of a compound and the published values on human plasma protein binding and blood-to-plasma concentration ratio (C_{blood}/C_{plasma}).

Hepatocytes in 12-well plates were preloaded until a maximal intracellular concentration was reached, as described for the uptake experiments. Measuring the compound efflux at maximal intracellular concentration gives the efflux at steady state. Preload times and compound concentrations were decided from measured uptake data in pilot experiments (digoxin, 10 μM for 15 minutes; fexofenadine, 1 μM for 30 minutes; napsagatran, 10 μM for 30 minutes; and rosuvastatin, 1 μM for 15 minutes). After preloading, the wells were washed three times in 37°C KHL to ensure that the wells were free from remaining compound. Efflux experiments were started by adding 300 μl KHL (37°C) to each well. Cells were also lysed immediately after washing to determine the initial intracellular concentrations at the start of the experiment. The contribution of ABC-efflux transporter activity to the measured efflux was assayed using 0.5 μM of the inhibitors elacridar (GF120918, *N*-4-[2-(1,2,3,4-tetrahydro-6,7-dimethoxy-2-isoquinolinyl)ethyl]-phenyl)-9,10-dihydro-5-methoxy-9-oxo-4-acridine carboxamide hydrochloride), a P-gp and BCRP inhibitor, and fumitremorgin C (FTC), a BCRP inhibitor.

Triplicate wells from uptake and efflux experiments were lysed with 200 μl 1% SDS, and the protein concentration was determined with the BCA protein assay kit (Pierce Biotechnology/ThermoFischer Scientific, Rockford, IL). The hepatocyte number per well was calculated using published data (Sohlenius-Sternbeck, 2006).

Determination of Plasma Protein Binding. Plasma protein binding was determined by equilibrium dialysis. Rat plasma was mixed with the compound at a concentration of 10 μM (in 0.1% DMSO). A volume of 180 μl 0.122 M phosphate buffer, pH 7.4, and 75 mM NaCl was added to each well on one side of a dialysis plate, and 180 μl of the plasma/compound mix to the opposite side, separated by a dialysis membrane (Spectra/Por MWCO 6-8000; Spectrum Laboratories, Rancho Dominguez, CA). After incubation on an orbital shaker at 37°C for 18 hours, the samples were analyzed by LC-MS/MS. All compounds were stable during the 18-hour incubation.

Determination of Blood-to-Plasma Concentration Ratio (C_{blood}/C_{plasma}). The C_{blood}/C_{plasma} was determined in fresh rat whole blood for digoxin, fexofenadine, napsagatran, rosuvastatin, and midazolam (positive control). Two blood samples were spiked with 0.2 μM test compound and incubated on a waddling mixer at 37°C for 1 hour. The blood was centrifuged, and the resulting plasma was analyzed by LC-MS/MS.

Plasma Clearance of Test Compound. Blood samples were drawn from male Sprague-Dawley rats aged approximately 8 weeks just before and at 1, 5, 20, and 40 minutes, and at 1, 1.5, 3, 6, and 24 hours after intravenous bolus administration of 3 μmol/kg of test compound (in 0.3 M *N*-methyl-D-glucamine). Standards and samples were diluted in blank plasma and analyzed by LC-MS/MS.

Bile Clearance of Test Compound. Male Sprague-Daley rats aged approximately 8 weeks were anesthetized with isoflurane (Abbott) by use of a vaporizer and were then surgically prepared with a bile-pancreatic catheter (constructed by polyethylene catheter Physiocath and P90; Data Sciences International, St. Paul, MN). A small incision was made in the duodenum, and the catheter was inserted for the recycling of bile. A skin incision was made in the scapula region. A loop of the catheter was subcutaneously tunneled from the abdominal incision to the scapula region and was then secured with a draconic button.

After 3 days' recovery, the animals were connected to a swivel system (Instech Laboratories, Plymouth Meeting, PA) that allowed freedom of movement during the experiment; they were then administered a bolus dose of 3 μmol/kg of compound via a lateral caudal vein. Fractions of bile were collected every 10 minutes for the first hour and every hour until 6 hours after dosing. Plasma was drawn at 6 hours after dosing. The animals were finally sacrificed with an overdose of the barbiturate pentobarbital, veterinary grade (Apoteket Produktion & Laboratorier AB, Kungens Kurva, Sweden). Standards and samples were diluted in a 1:10 dilution of blank bile and analyzed by LC-MS/MS.

LC-MS/MS Analysis. Analysis of parent compounds and metabolites was performed by LC-MS/MS using a Micromass Quattro Micro triple quadrupole (Micromass, Manchester, United Kingdom). The software MassLynx was used to control the liquid chromatography system and mass spectrometer (Waters Corporation, Milford, MA). A high purity C_{18} 5 μm 30 × 2.1 mm (Thermo Electron Corporation, Waltham, MA) analytical column was used. A standard curve was included for each compound analyzed, spanning a concentration range from twice the initial experimental concentration to below the limit of quantification. The limit of quantification, the signal to noise ratio for detection, was set to 5 times.

Pharmacokinetics and IVIVE

Determination of In Vitro Intrinsic Clearance. The elimination rate constant in metabolic stability and uptake experiments was calculated from the first-order elimination equation:

$$[S] = [S_0] \cdot e^{-k \cdot t} \quad (1)$$

where $[S]$ is concentration of substrate at a given time point t, $[S_0]$ is the initial concentration of substrate, and k is the elimination rate constant, which was determined by nonlinear regression within a time point interval representing the initial elimination rate (Soars et al., 2007). For in vitro efflux, k is given by the rate of compound effluxed into the medium.

In vitro intrinsic clearances ($CL_{int,met}$, $CL_{int,uptake}$, $CL_{int,efflux}$) for the compounds could then be calculated from:

$$CL_{int} = k \cdot V \quad (2)$$

where V represents the volume of incubation. $CL_{int,efflux}$ is calculated using the volume and concentration of the preloading medium. This is the rate of efflux back into the medium when uptake experiments have reached steady state.

Intrinsic hepatic clearance according to the extended clearance concept incorporating both transport and metabolism is given by:

$$CL_{int,all} = CL_{int,uptake} \times \frac{(CL_{int,efflux} + CL_{int,met})}{(CL_{int,efflux} + CL_{int,met} + CL_{int,back})} \quad (3)$$

(Maeda and Sugiyama, 2010). $CL_{int,uptake}$ is the uptake CL_{int}, $CL_{int,efflux}$ is the efflux of compound from hepatocytes to bile, $CL_{int,met}$ is the metabolic CL_{int}, and $CL_{int,back}$ is the basolateral efflux from hepatocytes back to the circulation. Our in vitro efflux experiments cannot distinguish $CL_{int,efflux}$ and $CL_{int,back}$, so $CL_{int,back}$ was arbitrarily set to 0 for these experiments to allow calculations (see *Discussion* for further details).

When $CL_{int,back} = 0$, we have a compound with no sinusoidal active efflux and little passive permeability (i.e., a BDDCS class III or IV compound without sinusoidal active efflux) (Benet et al., 2011). All biliary probe compounds in this study are BDDCS class III compounds with unknown sinusoidal active efflux. $CL_{int,all}$ is in this case determined by the hepatocyte uptake:

$$CL_{int,all} = CL_{int,uptake} \quad (4)$$

However, in our in vitro experiments efflux is active, and the measured uptake is an apparent uptake diminished by the active efflux of the compound back into the medium. To compensate for this, the total uptake CL_{int} is calculated:

$$CL_{int,all} = CL_{int,uptake,total} = CL_{int,uptake} + CL_{int,efflux} \quad (5)$$

This equation gives the uptake rate that would be seen after complete inhibition of active efflux.

Fraction Unbound in the Incubations. The fraction unbound (fu) in the hepatocyte incubation was predicted according to Kilford et al. (2008):

$$fu_{inc,hep} = \frac{1}{1 + 125 \times V_R \times 10^{0.072 \times \log P/D^2 + 0.067 \times \log P/D - 1.126}} \quad (6)$$

where V_R is the ratio between the cell volume and the incubation volume with a value of 0.005 at the cell concentration 10^6 cells/ml. Log P is used for bases, and log D for other ion classes. Predicted log P and log D values were generated using a commercial package from Advanced Chemistry Development (Toronto, Canada).

TABLE 1

A comparison of metabolic CL_{int} for several phase I and II metabolic substrates in plated rat hepatocytes and suspended cells.

Substrate	BDDCS Class[a]	Main Metabolic Enzyme[b]	$CL_{int,met}$ (μl/min × 10^6 cells)	
			Plated Cells	Suspended Cells
Bufuralol	I	CYP2D2	64 ± 12	68 ± 9
Diazepam	I	CYP2C11	24 ± 6	34 ± 8
Diclofenac	I	CYP2C6	23 ± 5	26 ± 6
7-Hydroxycoumarin	I	UGT	38 ± 24	53 ± 7
Midazolam	I	CYP3A	40 ± 9	45 ± 8
Phenacetin	II	CYP1A2	29 ± 4*	39 ± 11

Mean +/− S.D. is shown, n = 3 for plated cells, >100 for suspended cells (long-term laboratory average). Statistical significance was tested with the two-tailed Student's t test. *P < 0.05, significantly lower than in suspended hepatocytes.

[a]BDDCS classes as described by Benet et al. (2011).

[b]Rat CYP isoform specificities were from Kobayashi et al. (2002).

Determination of In Vivo Clearance. In vivo blood clearance was calculated according to

$$CL_{blood} = \frac{Intravenous\ Dose}{AUC_{blood}} \quad (7)$$

where

$$AUC_{blood} = \frac{AUC_{plasma} \times C_{blood}}{C_{plasma}} \quad (8)$$

The blood-to-bile CL was calculated with the equation:

$$CL_{bile} = \frac{X_{t1-t2}}{AUC_{blood,t1-t2}} \quad (9)$$

where $X_{t1–t2}$ denotes the amount secreted in bile between the two time points and $AUC_{blood,t1–t2}$ is the blood area under the concentration-time curve (AUC) for the same time interval (Fukuda et al., 2008). In this study, the time interval spans the first hour after intravenous administration of compound.

In vivo hepatic clearance, $CL_{hepatic}$, is calculated according to:

$$CL_{hepatic} = CL_{blood} \times f_{hepatic} \quad (10)$$

where the hepatic fraction, $f_{hepatic}$, for the biliary cleared test compounds is given in the literature (Lavé et al., 1999; Kamath et al., 2005; Yang et al., 2009). $CL_{hepatic}$ comprises both metabolic and biliary efflux clearances.

Calculation of Fraction Unbound in the Blood. The fraction unbound in the blood (fu_{blood}) was calculated using the following equation:

$$fu_{blood} = \frac{fu_{plasma}}{(C_{blood}/C_{plasma})} \quad (11)$$

Prediction of In Vivo CL_{int}. The predicted $CL_{int,in\ vivo}$ for the liver was calculated as follows:

$$Predicted\ CL_{int\ in\ vivo} = \frac{CL_{int\ in\ vitro} \times physiological\ scaling\ factors \times fu_{blood}}{fu_{inc,hep}} \quad (12)$$

The physiologic scaling factors for rat hepatocytes were: (120 × 10^6 cells/g liver) × (10 g liver/250 g body weight) (Bayliss et al., 1990; Sohlenius-Sternbeck 2006). $CL_{int,in\ vitro}$ can be either $CL_{int,uptake}$, $CL_{int,efflux}$, $CL_{int,met}$ (all from eq. 2), or $CL_{int,uptake,total}$ (eq. 3 to eq. 5), which are then used to predict $CL_{hepatic}$ or CL_{bile} using eq. 13.

Prediction of In Vivo CL from In Vitro Data. Predictions were based on the well-stirred model:

TABLE 2

Comparison of uptake rates ($CL_{int,uptake}$) for plated rat hepatocytes and suspended cells.

Substrate	BDDCS Class[a]	Uptake Transporter[b]	$CL_{int,uptake}$ (μl/min × 10^6 cells)	
			Plated Cells	Suspended Cells
Atenolol[c]	III	None	1.2 ± 0.2***	3.9 ± 0.4
Metoprolol[c]	I	None	10 ± 2**	27 ± 3
Atorvastatin	II	OATPs	30 ± 3	30 ± 4
Bosentan	II	OATPs	11.5 ± 3	18 ± 3
Estrone-3-sulfate[d]	III	NTCP/OATs/OATPs	75 ± 9**	210 ± 32
Fexofenadine	III	OATPs	3 ± 0.5**	6 ± 1
Terfenadine[c]	II	None	153 ± 19**	324 ± 53
Montelukast	II	OATPs	145 ± 20	143 ± 14

Mean 6 S.D. is shown, n = 3. Statistical significance was tested with the two-tailed Student's t test. ** P < 0.01, *** P < 0.001.

[a]BDDCS class as described by Benet et al. (2011).

[b]Transporter data are from the University of Tokyo and University of California–San Francisco and U.S. Food and Drug Administration (UCSF-FDA) online transporter databases (Ozawa et al., 2004; Morrissey et al., 2012); http://bts.ucsf.edu/fdatransportal.

[c]Compounds with predominantly passive uptake.

[d]As no dose value can be assigned to estrone-3-sulfate, no true BDDCS class assignation can be given, except to note that it is a highly soluble compound with little passive permeability.

$$Predicted\ CL_{hepatic}\ or\ CL_{bile} = \frac{Q_{h,b} \times CL_{int,in\ vivo}}{(Q_{h,b} + CL_{int,in\ vivo})} \quad (13)$$

Hepatic blood flow, $Q_{h,b}$, was set to 72 ml/min/kg for the rat (Brown, et al., 1997). CL_{bile} was predicted from $CL_{int,efflux}$, and $CL_{hepatic}$ was for comparative purposes predicted from $CL_{int,met}$, $CL_{int,uptake}$, and $CL_{int,uptake,total}$ (using eq. 12 and eq. 13).

Statistical Analysis. Data were analyzed using GraphPad Prism 5 software (GraphPad Software, La Jolla, CA). Data are given as mean ± S.D. Statistical significance was tested using the two-tailed Student's *t* test (*$P < 0.05$; ** = $P < 0.01$; *** = $P < 0.001$). $P < 0.05$ was considered statistically significant.

Results

Plating of Hepatocytes. After plating, the hepatocytes formed a loosely confluent layer exhibiting a cobblestone appearance (data not shown). Experiments started within 4 hours of liver collagenase perfusion, including 90 minutes of plating.

Metabolism and Uptake in Plated Cells. A range of highly permeable BDDCS class I and II compounds (Benet et al., 2011), known to be metabolized by CYP and UGT enzymes, were used to assess drug metabolic capacity in plated and suspended rat hepatocytes. The results presented in Table 1 indicate that short-term plated hepatocytes retain similar metabolic capacity as freshly isolated cells.

Uptake rates for a number of well-characterized uptake substrates from high and low permeable BDDCS classes were compared in plated and suspended hepatocytes (Table 2). The $CL_{int,uptake}$ of atorvastatin, bosentan, and montelukast, which are predominantly dependent on transporters to be taken up by cells, was similar in plated and suspended hepatocytes. However, the uptake rates of estrone-3-sulfate and fexofenadine, well-known transporter substrates, were higher in suspended than in plated cells. Atenolol, metoprolol, and terfenadine, substances that are not known to be dependent on uptake transporters, also showed higher $CL_{int,uptake}$ in suspensions than in plated hepatocytes as a larger membrane area is exposed in the suspended cells. Cyclosporine A, a well-characterized OATP-inhibitor, efficiently inhibited atorvastatin uptake in plated hepatocytes (Supplemental Fig. 1A). In the absence of Na^+ a significant decrease of taurocholate uptake was observed, indicating NTCP activity in the plated hepatocytes (Supplemental Fig. 1B).

Temperature had a significant effect on uptake of atenolol, a drug that is passively taken up by the cell, reducing uptake 5-fold at 4°C as compared with 37°C (Supplemental Fig. 1C). As a consequence, low temperature uptake was not used as a negative control for active uptake in this study.

Properties of the Selected Test Set of Biliary Cleared Compounds. The selected biliary cleared compounds exhibited diverse clearance pathways and drug transporter involvement (Table 3). The compounds showed low to moderate plasma protein binding, diverse lipophilicities, and limited passive permeability (BDDCS class III) (Benet et al., 2011).

In Vitro Pharmacokinetic Properties of the Biliary Cleared Compounds. The compounds showed limited metabolic CL_{int} (Table 4). All compounds in the test set were taken up by plated rat hepatocytes (Table 4). Efflux measurements for all compounds were performed after preloading when the compound had reached a maximal intracellular concentration.

The decreasing intracellular amount and efflux of compound from the cells into the medium was measured as illustrated in Fig. 1, A and B, for rosuvastatin. $CL_{int,efflux}$ values for the tested compounds are given in Table 4. The measured $CL_{int,efflux}$ values were 0.13 ± 0.06, 3.2 ± 0.6, 10.1 ± 2.3, and 110 ± 2.8 for digoxin, fexofenadine, napsagatran, and

TABLE 3
In vivo and in vitro properties of the biliary cleared test set.

	BDDCS class[a]	Clearance mechanism[b]		Uptake transporters[c]		Efflux transporters[c]		Rat plasma protein binding (fu_{plasma})	Cblood/Cplasma	Chemical Class (N/Z/A/B)[e]	clogD7.4
		Human	Rat	Human	Rat	Human	Rat				
Digoxin	III	Renal > biliary	Metabolic > renal > biliary	OATP1B1 OATP1B3 Unknown[d]	OATP1-family OATP2B1	P-gp MDR3	P-gp	0.84	1.2	N	0.9
Fexofenadine	III	Biliary > renal	Biliary > renal	OATP1A2 OATP1B3 OATP2B1 OAT3	OATP1A-family OATP2B1	P-gp MRP2 MRP3	P-gp MRP2 ?	0.27	1.0	Z	2.3
Napsagatran	III	Biliary > renal	Biliary > renal	?	?	?	?	0.87	0.6	Z	−2.2
Rosuvastatin	III	Biliary > renal > metabolic	Biliary > renal > metabolic	NTCP OATP1B1 OATP1B3 OATP2B1 OAT3	OATP1A-family OATP1B2 OATP2B1	BCRP MRP2	BCRP MRP2	0.1	0.6	A	−2.7

[a]BDDCS classes as described by Benet et al. (2011).
[b]Clearance mechanisms are given in Kamath et al., 2005; Lavé et al., 1999; Poirier et al., 2009; Yang et al., 2009.
[c]Transporter data are from the University of Tokyo and University of California–San Francisco and U.S. Food and Drug Administration (UCSF-FDA) online transporter databases (Ozawa et al., 2004; Morrissey et al., 2012); http://bts.ucsf.edu/fdatransportal.
[d]The involvement of OATPs in digoxin uptake has recently come under debate; an alternative, as-yet-unidentified, sodium-dependent transporter has been proposed (Taub et al., 2011).
[e]Chemical class: N, neutral; Z, Zwitterion; A, acid; B, base.

TABLE 4

Rat in vitro and in vivo pharmacokinetics and in vitro–in vivo extrapolation of rat clearance for the biliary cleared compound set.

Rat In Vitro PK	$CL_{int,met}$ Microsome[a]	$CL_{int,met}$ Hepatocyte[a]	$CL_{int,uptake}$	$CL_{int,efflux}$	$CL_{int,uptake,total}$[b]	In Vitro Efflux
	μl/min/mg protein		*μl/min/10^6 hepatocytes*			*pmol/min/well*
Substrate						
Digoxin	10 ± 2.8	7 ± 1.5	3 ± 0.5	0.6 ± 0.2	3.6 ± 0.9	0.13 ± 0.06
Fexofenadine	6 ± 1.1	<5	3 ± 0.6	3.2 ± 0.4	6.2 ± 1.3	3.2 ± 0.6
Napsagatran	14 ± 5.2	5 ± 0.8	2.2 ± 0.4	4.8 ± 0.8	7 ± 1.6	10.1 ± 2.3
Rosuvastatin	6 ± 1.8	<5	11 ± 1.5	73.6 ± 5	84.6 ± 7.4	110 ± 28

Rat In Vivo PK	CL_{blood}[c]	$CL_{hepatic}$[d]	CL_{bile}[e]	Biliary Efflux
		ml/min/kg		*nmol/min/kg*
Substrate				
Digoxin	4.8 ± 2.2	3.4	0.8 ± 0.3	0.31 ± 0.1
Fexofenadine	10.9 ± 3.4	7.2	3.5 ± 0.6	20.9 ± 2.4
Napsagatran	35.5 ± 5.6	24.8	9 ± 2.4	14.6 ± 2
Rosuvastatin	62.8 ± 8.2	50	48 ± 10.8	100.6 ± 33

Rat IVIVE	Predicted CL_{bile} from $CL_{int,efflux}$[f]	Fold Error CL_{bile}[g]	Predicted $CL_{hepatic}$ from $CL_{int,uptake}$[h]	Fold Error $CL_{hepatic}$[g]	Predicted $CL_{hepatic}$ from $CL_{int,uptake,total}$[h]	Fold Error $CL_{hepatic}$[g]
	ml/min/kg		*ml/min/kg*		*ml/min/kg*	
Substrate						
Digoxin	1.1 ± 0.4	1.3	5.2 ± 0.8	1.6	6.1 ± 1.5	1.8
Fexofenadine	2.6 ± 0.3	1.4	2.4 ± 0.5	3	4.8 ± 0.9	1.5
Napsagatran	15.5 ± 1.4	1.7	8.4 ± 1.3	3	20.0 ± 2.8	1.3
Rosuvastatin	21.8 ± 1	2.2	4.9 ± 0.6	10	23.6 ± 1.6	2.1
	Average fold error[g]	1.7		4.5		1.7

Mean +/− S.D. is shown, n = 3.
[a]The limit of quantification for intrinsic metabolism experiments was 5 μl/min/mg protein or 5 μl/min/10^6 hepatocytes.
[b]$CL_{int,uptake,total} = CL_{int,uptake} + CL_{int,efflux}$ (eq. 5).
[c]CL_{blood} was calculated according to eq. 7 and eq. 8.
[d]$CL_{hepatic}$ was calculated using eq. 10. The $f_{hepatic}$ data were taken from the literature (Lavé et al., 1999; Kamath et al., 2005; Yang et al., 2009).
[e]CL_{bile} denotes blood to bile CL (eq. 9).
[f]In vitro efflux measurements ($CL_{int,efflux}$) were extrapolated to in vivo CL_{bile} (eq. 12 and eq. 13).
[g]Absolute fold error and average absolute fold error are given for predictions.
[h]$CL_{hepatic}$ was predicted from $CL_{int,uptake}$ and $CL_{int,uptake,total}$ (eq. 12, and eq. 13).

rosuvastatin, respectively, thus representing drugs with a >800-fold range of efflux rates. As efflux in these experiments counteracts and diminishes uptake measurements, $CL_{int,uptake,total}$ was calculated according to eq. 5.

Efflux from plated rat hepatocytes could be inhibited by ABC-transporter inhibitors. Efflux of rosuvastatin could be inhibited with 0.5 μM FTC, an inhibitor of BCRP (Fig. 1C). Efflux of fexofenadine was reduced in the presence of 0.5 mM of the P-gp and BCRP inhibitor elacridar (Fig. 1D).

Rat In Vivo Pharmacokinetics. Rat in vivo blood and biliary CL were determined in three animals for each of the four biliary cleared compounds (Table 4). All compounds were rapidly excreted into bile. The rates of biliary clearance varied 60-fold between digoxin and rosuvastatin (Table 4). For all compounds, the concentration in bile peaked 20 minutes after intravenous administration of compound. Peak bile concentrations varied from 4 μM for digoxin to 3000 μM for rosuvastatin. The fraction of the given dose recovered in the bile during 3 hours varied from 10% for digoxin over napsagatran (20%) and fexofenadine (29%) to 85% for rosuvastatin.

Bile flow was similar between animals and over time during the collection period (28 ± 5 μl/min, mean ± S.D., $n = 8$). There was no correlation between bile flow and secretion rate or between bile flow and the amount of compound excreted in bile.

Biliary CL (CL_{bile}) was calculated according to eq. 9 (Fukuda et al., 2008) and is presented in Table 4. Biliary CL constituted a significant portion of the clearance of all tested compounds. In vitro efflux and in vivo CL_{bile} showed the same rank order of rosuvastatin > napsagatran > fexofenadine > digoxin (Table 4).

In Vitro–In Vivo Extrapolation. When $CL_{hepatic}$ was predicted from hepatocyte or microsomal metabolic $CL_{int,met}$ using the well-stirred model (eq. 12 and eq. 13; Table 4), an absolute average fold error of more than 10-fold was obtained, and the slope of the best fit line was not significant (data not shown).

The CL_{bile} of digoxin, fexofenadine, napsagatran, and rosuvastatin was well predicted from $CL_{int,efflux}$ using the well-stirred model (eq. 12 and eq. 13; Table 4). Extrapolations showed an even distribution of over-predictions and underpredictions and an absolute average fold error of 1.7. Digoxin, fexofenadine, and napsagatran CL_{bile} was predicted within 2-fold of measured in vivo values, while the prediction for rosuvastatin showed an error of 2.2-fold (Table 4). The best fit line of the IVIVE data showed $r^2 = 0.89$, and its slope was significantly different from 0 (Fig. 2A).

The results from our present study indicate that scaling $CL_{hepatic}$ of digoxin, fexofenadine, napsagatran, and rosuvastatin from plated rat hepatocyte $CL_{int,uptake}$ (eq. 12 and eq. 13; Table 4) consistently underpredicted in vivo observations with errors ranging from 1.6- to 10-fold. The best fit line was not significantly different from 0 (Fig. 2B; Table 4).

Because active efflux in the plated hepatocytes will affect uptake measurements, $CL_{int,uptake,total}$ was calculated according to eq. 5

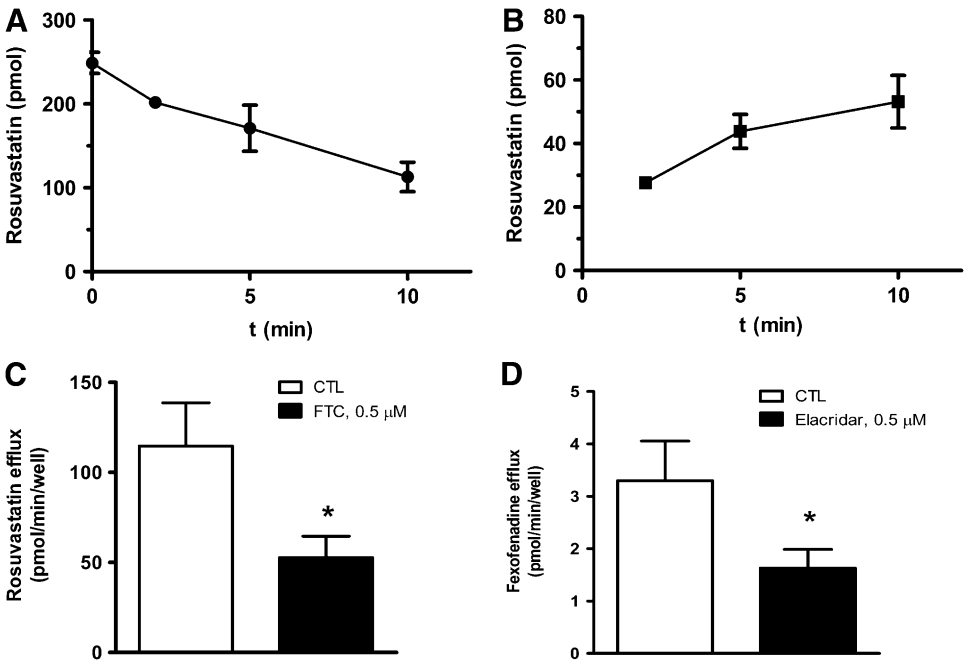

Fig. 1. Efflux of rosuvastatin and fexofenadine from plated rat hepatocytes. (A) Rosuvastatin remaining in the cell layer. (B) Accumulation of rosuvastatin in efflux media. (C) Efflux of rosuvastatin could be significantly reduced by addition of the BCRP inhibitor FTC. (D) Efflux of fexofenadine from plated rat hepatocytes is diminished in the presence of the P-gp and BCRP inhibitor elacridar. CTL, control experiment, standard conditions. (Mean ± S.D., $n = 3$, $^*P < 0.05$.)

(Table 4). This compensates for reductions in measured uptake due to active efflux from the hepatocytes. $CL_{hepatic}$ was again predicted, now from $CL_{int,uptake,total}$ (eq. 12 and eq. 13; Table 4). The predictions were significantly improved. Three out of four compounds were slightly underpredicted. Predictions of $CL_{hepatic}$ for digoxin, fexofenadine, and napsagatran were within 2-fold of observed in vivo values, whereas the prediction for rosuvastatin showed an error of 2.1-fold. The absolute average fold error of the predictions was 1.7 (Table 4). The best fit line of the IVIVE data showed an $r^2 = 0.84$, and its slope was significantly different from 0 (Fig. 2C).

Discussion

Short-term plated hepatocytes have previously been used for kinetic characterization and modeling of hepatic drug uptake and metabolism, but little attention has been paid to the impact of active efflux in the system (Menochet et al., 2012a, b). The active efflux component may have a major influence on cellular kinetics and thus merits further investigation. As demonstrated in our study, active efflux of digoxin, fexofenadine, napsagatran, and rosuvastatin in short-term plated rat hepatocytes predicts biliary clearance within 2-fold, and inclusion of the efflux component in IVIVE of hepatic clearance from in vitro uptake data improved predictions considerably.

Rat CL_{bile} rates of digoxin, fexofenadine, napsagatran, and rosuvastatin as predicted from in vitro efflux data from plated rat hepatocytes were not related to a general underprediction of the studied compounds as often experienced using other in vitro systems. Earlier attempts to scale rat in vivo CL_{bile} from rat SCH efflux, incorporating fu_{blood}, for the biliary cleared compound set resulted in 1.6-fold (digoxin), 3.5-fold (fexofenadine), and 15- to 17-fold (rosuvastatin) underpredictions (Annaert et al., 2001; Turncliff et al., 2006; Fukuda et al., 2008; Nakakariya et al., 2012). Nakakariya et al. (2012) have recently shown that biliary clearance predictions from rat SCH can be considerably improved by predicting biliary intrinsic clearance using liver tissue drug concentrations and free intracellular concentrations in rat SCH. Predicting rat CL_{bile} using rat SCH efflux in the traditional manner yielded underpredictions ranging from 7-fold to 300-fold. Predicting intrinsic biliary efflux using intracellular SCH and liver concentrations improved the results, giving underpredictions with an average fold error of 4.5, representing the most successful in vitro method to date for the prediction of biliary clearance (Nakakariya et al., 2012).

Although a few previous studies have suggested that isolated rat hepatocytes lose part of their ABC transporters (Bow et al., 2008), others have demonstrated both expression and activity of efflux transporters in freshly isolated rat hepatocytes (Lam et al., 2006; Li et al., 2008, 2009a,b,c). In a recent study, we demonstrated retained protein levels, membrane localization, and activity for rBCRP, rP-gp, and rMRP2 in freshly isolated rat hepatocytes as well as cryopreserved human hepatocytes (Lundquist et al., 2014a). In our present study, efflux from preloaded rat hepatocytes could be inhibited with well-characterized ABC efflux transporter inhibitors, indicating that rBCRP and rP-gp are active in short-term cultured hepatocytes.

Despite the compounds being cleared by a wide range of mechanisms and being substrates of many different transporters as listed in Table 3, the prediction errors were similar for all compounds tested. Investigation of bile clearance using the in vitro model proposed in our study will best predict in vivo biliary clearance for compounds exhibiting limited sinusoidal efflux, low passive permeability, and low lipophilicity/low unspecific cellular binding. These are characteristics shared by many compounds with pronounced biliary clearance (Yang et al., 2009). Short-term cultures of human cryopreserved hepatocytes should be investigated in future studies to help improve predictions of human biliary clearance. However, the pronounced down-regulation of OATP transporters that was recently demonstrated in human cryopreserved hepatocytes might present a limitation (Kimoto et al., 2012; Lundquist et al., 2014b).

Scaling $CL_{hepatic}$ from plated rat hepatocyte uptake data, the in vivo values were consistently underpredicted in our present study. Similar results were obtained by Gardiner and Paine (2011), who noted a 6-fold underprediction from rat hepatocyte uptake data. Menochet et al. (2012b) also presented underpredictions of in vivo hepatic uptake from in vitro uptake measurements using rat hepatocytes. As can be seen in Table 4 and Fig. 2B, the underprediction of $CL_{hepatic}$ from plated hepatocyte uptake data became larger for compounds with

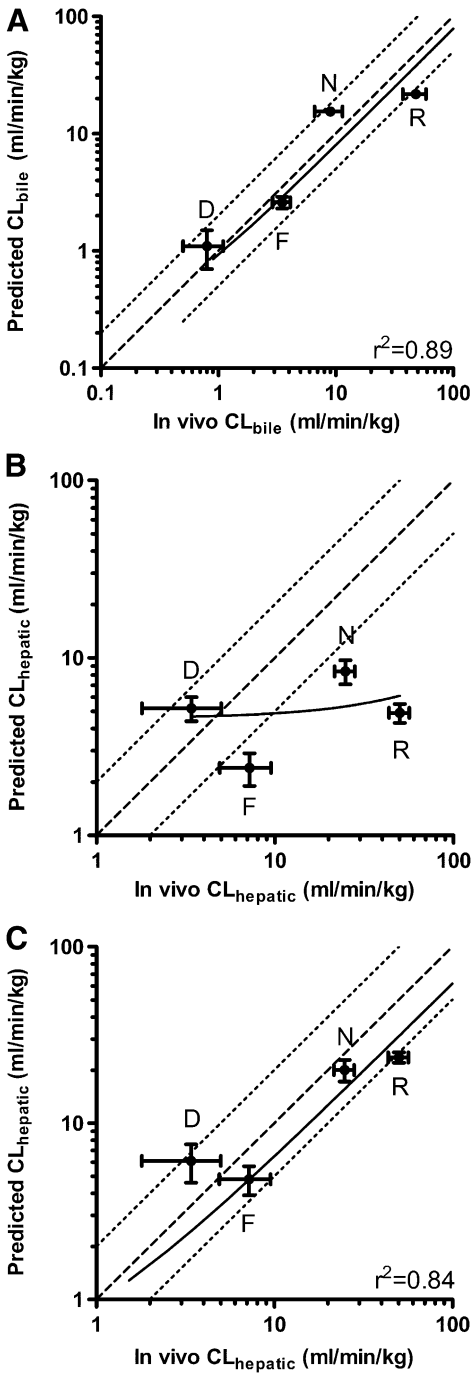

Fig. 2. In vitro–in vivo extrapolation of rat PK from Table 4. (A) Prediction of in vivo CL_{bile} from plated hepatocyte $CL_{int,efflux}$. (B) Prediction of in vivo $CL_{hepatic}$ from plated hepatocyte $CL_{int,uptake}$. (C) Prediction of in vivo $CL_{hepatic}$ from plated hepatocyte $CL_{int,uptake,total}$. The line of unity between extrapolation and observation as well as lines representing 2-fold errors are shown by dotted lines. The best fit line from linear regression is represented by a solid line with an r^2 = 0.89 and a significant slope ($P < 0.05$) for 6A. The best fit line in 6C shows an r^2 = 0.84 and a significant slope ($P < 0.05$). D, digoxin; F, fexofenadine; N, napsagatran; R, rosuvastatin. (Mean ± S.D., n = 3.)

higher efflux rates. In the study by Menochet et al. (2012b), rosuvastatin needed the largest correction factor and is also the compound with the highest CL_{bile} and in vitro efflux.

Due to active efflux from the hepatocytes, the true cellular uptake is probably underestimated. We recently showed that the apparent fexofenadine uptake in rat hepatocytes increased more than 4-fold when inhibiting P-gp during the uptake experiment (Lundquist et al., 2014b), supporting this hypothesis. As clearly shown in our present study, compensating for active efflux in the plated hepatocytes by calculating $CL_{int,uptake,total}$ (eq. 5) significantly improved the IVIVE of $CL_{hepatic}$.

The loss of polarity of the isolated hepatocytes used in cell suspension or short-term cultures results in both basolateral (sinusoidal, facing the circulation) and apical (canalicular, facing the bile) efflux transporters exporting compound into the same medium compartment. The presence of sinusoidal efflux could therefore lead to overprediction of biliary CL for certain compounds because the measured $CL_{int,efflux}$ will be overestimated and contain both canalicular and sinusoidal efflux. As can be inferred from eq. 3, biliary efflux will be overpredicted by a factor of 2 if sinusoidal and canalicular efflux are of the same magnitude ($CL_{int,efflux} = CL_{int,back}$).

Little is known of basolateral efflux for the study compounds. Digoxin is an OSTα-OSTβ substrate (Seward et al., 2003), but nothing is known of its in vivo significance. Fexofenadine is a MRP3 substrate in mouse liver where sinusoidal and basolateral fexofenadine effluxes are of similar magnitude (Matsushima et al., 2008; Tian et al., 2008). Mice have been shown to express high levels of MRP3 compared with rats, where basolateral efflux thus might be less pronounced (Chu et al., 2006). Likewise, rosuvastatin has recently been shown to exhibit similar basolateral and canalicular efflux in rat SCH, after the large up-regulation of rMRP3 and rMRP4 taking place in rat SCH (Pfeifer et al., 2013). The error introduced by basolateral efflux in short-term plated rat hepatocytes is thus likely to be small for these compounds.

In the liver, most sinusoidal efflux transporters show low expression compared with the canalicular ones; MRP3 is barely detectable in rat liver and short-term hepatocyte cultures whereas MRP2 shows very high expression (Rippin et al., 2001; Luttringer et al., 2002). The expression of rMRP2 in rat liver is more than twice the combined levels of rMRP3 and rMRP4 (Rippin et al., 2001; Luttringer et al., 2002; Jigorel et al., 2005). It is known that for some drug metabolites, particularly sulfate conjugates, the sinusoidal efflux may be very high, but data on parent compounds are scarce, so this area merits further study (Zamek-Gliszczynski et al., 2006). In the present study, CL_{bile} was not overpredicted when scaling from in vitro $CL_{int,efflux}$, and the rank orders for in vitro efflux and CL_{bile} were identical, suggesting that basolateral efflux was not a major component in the efflux of the tested compounds.

Compounds with high passive permeability may also present a problem in the experimental model as this component may be difficult to determine experimentally. The biliary cleared compound set used consists of low permeable BDDCS class III compounds (Lavé et al., 1999; Benet et al., 2011). For rosuvastatin and fexofenadine, the passive uptake component has been estimated to be less than 10% of the total hepatocyte uptake and is thus unlikely to have a major impact on measurements (Menochet et al., 2012a).

In conclusion, we have developed an experimental technique based on short-term plated hepatocytes that allows the measurement of uptake, metabolism, and efflux of drug compounds. Basolateral efflux is, however, not considered and may introduce errors into the predictions. In vitro efflux measurements using this model predicted biliary clearance within or close to 2-fold of measured in vivo values for four compounds—digoxin, fexofenadine, napsagatran, and rosuvastatin—that exhibit a wide range of in vivo biliary clearances. Efflux-corrected in vitro uptake measurements were used to improve the IVIVE of hepatic CL. The short-term hepatocyte culture model described thus provides a simple way to study uptake, metabolic, and efflux clearance pathways in the liver of new chemical entities and

considerably improves the prediction of hepatic clearance, especially for compounds with a large biliary clearance component.

Acknowledgments

The authors thank Annelie Bengtsson, Jessie Dahlström, Eva Floby, and Stefan Martinsson for their great and generous help.

Authorship Contributions

Participated in research design: Lundquist, Lööf, Fagerholm, Sjögren, Briem, Johansson, Afzelius, Andersson.

Conducted experiments: Lundquist, Lööf, Sjögren, Briem, Johansson.

Contributed new reagents or analytic tools: Lundquist, Johansson, Briem, Fagerholm.

Performed data analysis: Lundquist, Lööf, Fagerholm.

Wrote or contributed to the writing of the manuscript: Lundquist, Fagerholm, Briem, Johansson, Hoogstraate, Afzelius, Andersson.

References

Annaert PP, Turncliff RZ, Booth CL, Thakker DR, and Brouwer KL (2001) P-glycoprotein-mediated in vitro biliary excretion in sandwich-cultured rat hepatocytes. *Drug Metab Dispos* **29**:1277–1283.

Bayliss MK, Bell JA, Jenner WN, and Wilson K (1990) Prediction of intrinsic clearance of loxtidine from kinetic studies in rat, dog and human hepatocytes. *Biochem Soc Trans* **18**: 1198–1199.

Beigel J, Fella K, Kramer PJ, Kroeger M, and Hewitt P (2008) Genomics and proteomics analysis of cultured primary rat hepatocytes. *Toxicol In Vitro* **22**:171–181.

Benet LZ, Broccatelli F, and Oprea TI (2011) BDDCS applied to over 900 drugs. *AAPS J* **13**: 519–547.

Bissell DM and Guzelian PS (1980) Phenotypic stability of adult rat hepatocytes in primary monolayer culture. *Ann N Y Acad Sci* **349**:85–98.

Bow DA, Perry JL, Miller DS, Pritchard JB, and Brouwer KL (2008) Localization of P-gp (Abcb1) and Mrp2 (Abcc2) in freshly isolated rat hepatocytes. *Drug Metab Dispos* **36**: 198–202.

Boyer JL, Trauner M, Mennone A, Soroka CJ, Cai SY, Moustafa T, Zollner G, Lee JY, and Ballatori N (2006) Upregulation of a basolateral FXR-dependent bile acid efflux transporter OSTα-OSTβ in cholestasis in humans and rodents. *Am J Physiol Gastrointest Liver Physiol* **290**:G1124–G1130.

Brown RP, Delp MD, Lindstedt SL, Rhomberg LR, and Beliles RP (1997) Physiological parameter values for physiologically based pharmacokinetic models. *Toxicol Ind Health* **13**: 407–484.

Chu XY, Strauss JR, Mariano MA, Li J, Newton DJ, Cai X, Wang RW, Yabut J, Hartley DP, and Evans DC, et al. (2006) Characterization of mice lacking the multidrug resistance protein MRP2 (ABCC2). *J Pharmacol Exp Ther* **317**:579–589.

De Bruyn T, Chatterjee S, Fattah S, Keemink J, Nicolaï J, Augustijns P, and Annaert P (2013) Sandwich-cultured hepatocytes: utility for in vitro exploration of hepatobiliary drug disposition and drug-induced hepatotoxicity. *Expert Opin Drug Metab Toxicol* **9**: 589–616.

Fukuda H, Ohashi R, Tsuda-Tsukimoto M, and Tamai I (2008) Effect of plasma protein binding on in vitro-in vivo correlation of biliary excretion of drugs evaluated by sandwich-cultured rat hepatocytes. *Drug Metab Dispos* **36**:1275–1282.

Gardiner P and Paine SW (2011) The impact of hepatic uptake on the pharmacokinetics of organic anions. *Drug Metab Dispos* **39**:1930–1938.

Giacomini KM, Huang SM, Tweedie DJ, Benet LZ, Brouwer KL, Chu X, Dahlin A, Evers R, Fischer V, and Hillgren KM, et al.; International Transporter Consortium (2010) Membrane transporters in drug development. *Nat Rev Drug Discov* **9**:215–236.

Gray KA, Daugherty LC, Gordon SM, Seal RL, Wright MW, and Bruford EA (2013) Genenames.org: the HGNC resources in 2013. *Nucleic Acids Res* **41** (Database issue): D545–D552.

Hagenbuch B and Stieger B (2013) The SLCO (former SLC21) superfamily of transporters. *Mol Aspects Med* **34**:396–412.

Jigorel E, Le Vee M, Boursier-Neyret C, Bertrand M, and Fardel O (2005) Functional expression of sinusoidal drug transporters in primary human and rat hepatocytes. *Drug Metab Dispos* **33**: 1418–1422.

Kamath AV, Yao M, Zhang Y, and Chong S (2005) Effect of fruit juices on the oral bioavailability of fexofenadine in rats. *J Pharm Sci* **94**:233–239.

Kilford PJ, Gertz M, Houston JB, and Galetin A (2008) Hepatocellular binding of drugs: correction for unbound fraction in hepatocyte incubations using microsomal binding or drug lipophilicity data. *Drug Metab Dispos* **36**:1194–1197.

Kimoto E, Yoshida K, Balogh LM, Bi YA, Maeda K, El-Kattan A, Sugiyama Y, and Lai Y (2012) Characterization of organic anion transporting polypeptide (OATP) expression and its functional contribution to the uptake of substrates in human hepatocytes. *Mol Pharm* **9**: 3535–3542.

Kobayashi K, Urashima K, Shimada N, and Chiba K (2002) Substrate specificity for rat cytochrome P450 (CYP) isoforms: screening with cDNA-expressed systems of the rat. *Biochem Pharmacol* **63**:889–896.

Kotani N, Maeda K, Watanabe T, Hiramatsu M, Gong LK, Bi YA, Takezawa T, Kusuhara H, and Sugiyama Y (2011) Culture period-dependent changes in the uptake of transporter substrates in sandwich-cultured rat and human hepatocytes. *Drug Metab Dispos* **39**:1503–1510.

Lam JL, Okochi H, Huang Y, and Benet LZ (2006) In vitro and in vivo correlation of hepatic transporter effects on erythromycin metabolism: characterizing the importance of transporter-enzyme interplay. *Drug Metab Dispos* **34**:1336–1344.

Lavé T, Portmann R, Schenker G, Gianni A, Guenzi A, Girometta MA, and Schmitt M (1999) Interspecies pharmacokinetic comparisons and allometric scaling of napsagatran, a low molecular weight thrombin inhibitor. *J Pharm Pharmacol* **51**:85–91.

Li M, Yuan H, Li N, Song G, Zheng Y, Baratta M, Hua F, Thurston A, Wang J, and Lai Y (2008) Identification of interspecies difference in efflux transporters of hepatocytes from dog, rat, monkey and human. *Eur J Pharm Sci* **35**:114–126.

Li N, Bi YA, Duignan DB, and Lai Y (2009a) Quantitative expression profile of hepatobiliary transporters in sandwich cultured rat and human hepatocytes. *Mol Pharm* **6**: 1180–1189.

Li N, Palandra J, Nemirovskiy OV, and Lai Y (2009b) LC-MS/MS mediated absolute quantification and comparison of bile salt export pump and breast cancer resistance protein in livers and hepatocytes across species. *Anal Chem* **81**:2251–2259.

Li N, Singh P, Mandrell KM, and Lai Y (2010) Improved extrapolation of hepatobiliary clearance from in vitro sandwich cultured rat hepatocytes through absolute quantification of hepatobiliary transporters. *Mol Pharm* **7**:630–641.

Li N, Zhang Y, Hua F, and Lai Y (2009c) Absolute difference of hepatobiliary transporter multidrug resistance-associated protein (MRP2/Mrp2) in liver tissues and isolated hepatocytes from rat, dog, monkey, and human. *Drug Metab Dispos* **37**:66–73.

Liu X, Brouwer KL, Gan LS, Brouwer KR, Stieger B, Meier PJ, Audus KL, and LeCluyse EL (1998) Partial maintenance of taurocholate uptake by adult rat hepatocytes cultured in a collagen sandwich configuration. *Pharm Res* **15**:1533–1539.

Liu X, LeCluyse EL, Brouwer KR, Lightfoot RM, Lee JI, and Brouwer KL (1999) Use of Ca^{2+} modulation to evaluate biliary excretion in sandwich-cultured rat hepatocytes. *J Pharmacol Exp Ther* **289**:1592–1599.

Luttringer O, Theil FP, Lavé T, Wernli-Kuratli K, Guentert TW, and de Saizieu A (2002) Influence of isolation procedure, extracellular matrix and dexamethasone on the regulation of membrane transporters gene expression in rat hepatocytes. *Biochem Pharmacol* **64**: 1637–1650.

Lundquist P, Englund G, Skogastierna C, Lööf J, Johansson J, Hoogstraate J, Afzelius L, and Andersson TB (2014a) Functional ATP-binding cassette drug efflux transporters in isolated human and rat hepatocytes significantly affect assessment of drug disposition. *Drug Metab Dispos* **42**: 441–447.

Lundquist P, Lööf J, Sohlenius-Sternbeck A-K, Floby E, Johansson J, Bylund J, Hoogstraate J, Afzelius L, and Andersson TB (2014b) The impact of solute carrier (SLC) drug uptake transporter loss in human and rat cryopreserved hepatocytes on clearance predictions. *Drug Metab Dispos* **42**: 469–480.

Maeda K and Sugiyama Y (2010) The use of hepatocytes to investigate drug uptake transporters. *Methods Mol Biol* **640**:327–353.

Matsushima S, Maeda K, Hayashi H, Debori Y, Schinkel AH, Schuetz JD, Kusuhara H, and Sugiyama Y (2008) Involvement of multiple efflux transporters in hepatic disposition of fexofenadine. *Mol Pharmacol* **73**:1474–1483.

Ménochet K, Kenworthy KE, Houston JB, and Galetin A (2012a) Simultaneous assessment of uptake and metabolism in rat hepatocytes: a comprehensive mechanistic model. *J Pharmacol Exp Ther* **341**:2–15.

Ménochet K, Kenworthy KE, Houston JB, and Galetin A (2012b) Use of mechanistic modeling to assess interindividual variability and interspecies differences in active uptake in human and rat hepatocytes. *Drug Metab Dispos* **40**:1744–1756.

Morrissey KM, Wen CC, Johns SJ, Zhang L, Huang SM, and Giacomini KM (2012) The UCSF-FDA TransPortal: a public drug transporter database. *Clin Pharmacol Ther* **92**: 545–546.

Nakakariya M, Ono M, Amano N, Moriwaki T, Maeda K, and Sugiyama Y (2012) In vivo biliary clearance should be predicted by intrinsic biliary clearance in sandwich-cultured hepatocytes. *Drug Metab Dispos* **40**:602–609.

Ozawa N, Shimizu T, Morita R, Yokono Y, Ochiai T, Munesada K, Ohashi A, Aida Y, Hama Y, and Taki K, et al. (2004) Transporter database, TP-Search: a web-accessible comprehensive database for research in pharmacokinetics of drugs. *Pharm Res* **21**: 2133–2134.

Pfeifer ND, Yang K, and Brouwer KL (2013) Hepatic basolateral efflux contributes significantly to rosuvastatin disposition I: characterization of basolateral versus biliary clearance using a novel protocol in sandwich-cultured hepatocytes. *J Pharmacol Exp Ther* **347**: 727–736.

Poirier A, Funk C, Scherrmann JM, and Lavé T (2009) Mechanistic modeling of hepatic transport from cells to whole body: application to napsagatran and fexofenadine. *Mol Pharm* **6**:1716–1733.

Rippin SJ, Hagenbuch B, Meier PJ, and Stieger B (2001) Cholestatic expression pattern of sinusoidal and canalicular organic anion transport systems in primary cultured rat hepatocytes. *Hepatology* **33**:776–782.

Seward DJ, Koh AS, Boyer JL, and Ballatori N (2003) Functional complementation between a novel mammalian polygenic transport complex and an evolutionarily ancient organic solute transporter, OSTα-OSTβ. *J Biol Chem* **278**:27473–27482.

Soars MG, Grime K, Sproston JL, Webborn PJ, and Riley RJ (2007) Use of hepatocytes to assess the contribution of hepatic uptake to clearance in vivo. *Drug Metab Dispos* **35**: 859–865.

Sohlenius-Sternbeck AK (2006) Determination of the hepatocellularity number for human, dog, rabbit, rat and mouse livers from protein concentration measurements. *Toxicol In Vitro* **20**: 1582–1586.

Sohlenius-Sternbeck AK, Afzelius L, Prusis P, Neelissen J, Hoogstraate J, Johansson J, Floby E, Bengtsson A, Gissberg O, and Sternbeck J, et al. (2010) Evaluation of the human prediction of clearance from hepatocyte and microsome intrinsic clearance for 52 drug compounds. *Xenobiotica* **40**:637–649.

Taub ME, Mease K, Sane RS, Watson CA, Chen L, Ellens H, Hirakawa B, Reyner EL, Jani M, and Lee CA (2011) Digoxin is not a substrate for organic anion-transporting polypeptide transporters OATP1A2, OATP1B1, OATP1B3, and OATP2B1 but is a substrate for a sodium-dependent transporter expressed in HEK293 cells. *Drug Metab Dispos* **39**: 2093–2102.

Tchaparian EH, Houghton JS, Uyeda C, Grillo MP, and Jin L (2011) Effect of culture time on the basal expression levels of drug transporters in sandwich-cultured primary rat hepatocytes. *Drug Metab Dispos* **39**:2387–2394.

Tian X, Swift B, Zamek-Gliszczynski MJ, Belinsky MG, Kruh GD, and Brouwer KL (2008) Impact of basolateral multidrug resistance-associated protein (Mrp) 3 and Mrp4 on the

hepatobiliary disposition of fexofenadine in perfused mouse livers. *Drug Metab Dispos* **36**:911–915.

Turncliff RZ, Hoffmaster KA, Kalvass JC, Pollack GM, and Brouwer KL (2006) Hepatobiliary disposition of a drug/metabolite pair: Comprehensive pharmacokinetic modeling in sandwich-cultured rat hepatocytes. *J Pharmacol Exp Ther* **318**:881–889.

Wu CY and Benet LZ (2005) Predicting drug disposition via application of BCS: transport/ absorption/ elimination interplay and development of a biopharmaceutics drug disposition classification system. *Pharm Res* **22**:11–23.

Yang X, Gandhi YA, Duignan DB, and Morris ME (2009) Prediction of biliary excretion in rats and humans using molecular weight and quantitative structure-pharmacokinetic relationships. *AAPS J* **11**:511–525.

Zamek-Gliszczynski MJ, Nezasa K, Tian X, Bridges AS, Lee K, Belinsky MG, Kruh GD, and Brouwer KL (2006) Evaluation of the role of multidrug resistance-associated protein (Mrp) 3 and Mrp4 in hepatic basolateral excretion of sulfate and glucuronide metabolites of acetaminophen, 4-methylumbelliferone, and harmol in Abcc3$^{-/-}$ and Abcc4$^{-/-}$ mice. *J Pharmacol Exp Ther* **319**:1485–1491.

Address correspondence to: Tommy B. Andersson, Cardiovascular and Metabolic Diseases Innovative Medicines DMPK, AstraZeneca R&D, Pepparedsleden 1, SE-431 83 Mölndal, Sweden. E-mail: tommy.b.andersson@astrazeneca.com